

## Chapter 7 Other phenomena\*

### 7.1 Sea ice

Major sea ice areas observed around Japan are the Sea of Okhotsk and near the Tatar Strait. Sea ice has about the same reflectance as cloud, so it appears in bright gray or gray on the visible image. Because the northern Sea of Okhotsk is situated in high latitudes and the elevation angle of the sun is low, the sea ice looks gray. The horizontal resolution around here is about 2 or 3 km, so the movements of sea ice can be kept track of. A sea ice area may be mistaken for a low cloud. However, because the moving speed is very slow compared with low cloud, distinction is easy on the moving image. Since the temperature difference with the surrounding sea surface temperature is small, distinction with the sea surface is difficult on the infrared image. Figure 7-1 shows an example of sea ice seen in the Sea of Okhotsk and the Tatar Strait. The sea ice touches the Shiretoko Peninsula and part of it is flowing out of a gap in the Kuril Islands (between Iturup and Kunashiri Islands) into the Pacific. General sea ice information is prepared using this data and it contributes much to safe navigation of vessels.

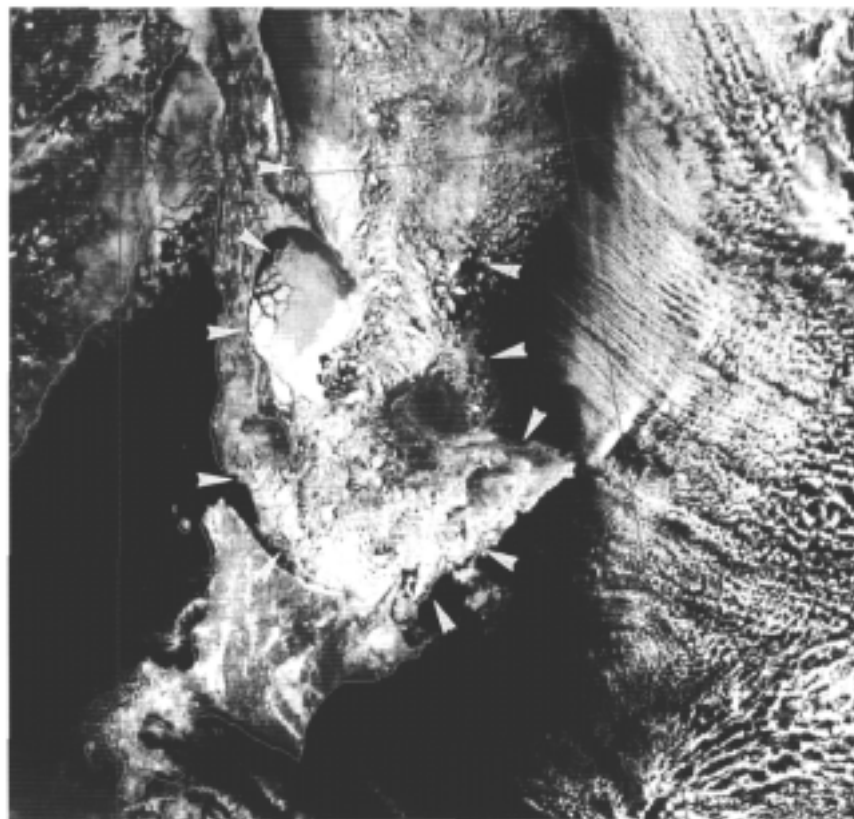


Figure 7-1. Visible image (gradation enhanced for brightness) at 01UTC, February 24, 1999  
Wedges: Sea ice

---

\* 7.1, 7.2, 7.7 Kou Egami, 7.3, 7.6, 7.8 Takeo Tanaka, 7.4, 7.5 Nobutoshi Fuchita

## 7.2 Snow cover

A snow cover has a high reflectance, so it is represented as a white region on the visible image. Identification is difficult on the infrared image because no temperature difference is seen with the surroundings. On the visible image, the snow cover surface is relatively smooth and looks the same for several days, so its distinction from a cloud area is possible. Figure 7-2-1 shows an example of snow cover areas seen in Hokkaido and on the Asian continent. The snow cover in Hokkaido is seen as a bright gray region nearly along the mountain ranges. The snow cover on the Asian continent looks gray on the western side because the elevation angle of the sun there is low compared with Hokkaido. On the other hand, Figure 7-2-2 shows an example of Kanto District. Because the snow cover areas are scattered, they appear as gray areas with an indistinct outline. The gray region around Tokyo (marked by an arrow) is a low cloud area superimposed on a snow cover area. This snow cover was brought about by a low that passed on the southern coast of Kanto District 2 days before, or 15th day. The deepest snow cover recorded at this case was 33 cm at Maebashi in northern Kanto District and 16 cm at Tokyo. The snow cover at 17th 00UTC was 24 cm at Maebashi and 8 cm at Tokyo.

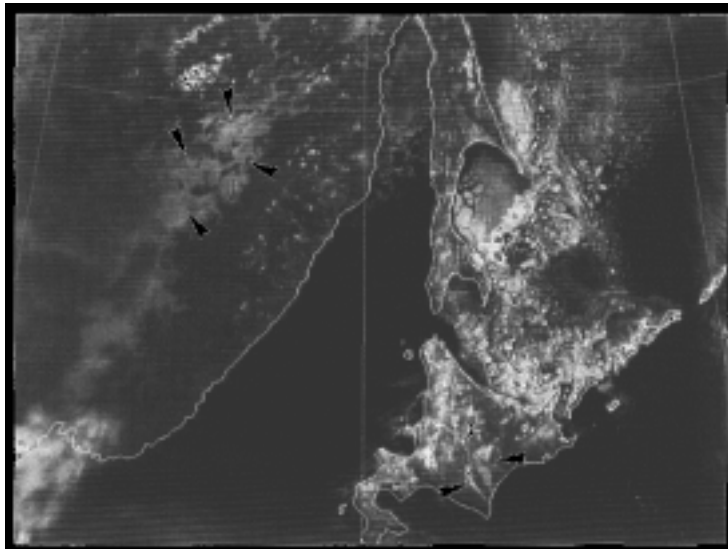


Figure 7-2-1. Visible image at 03UTC, February 24, 1999  
Wedges: Snow cover

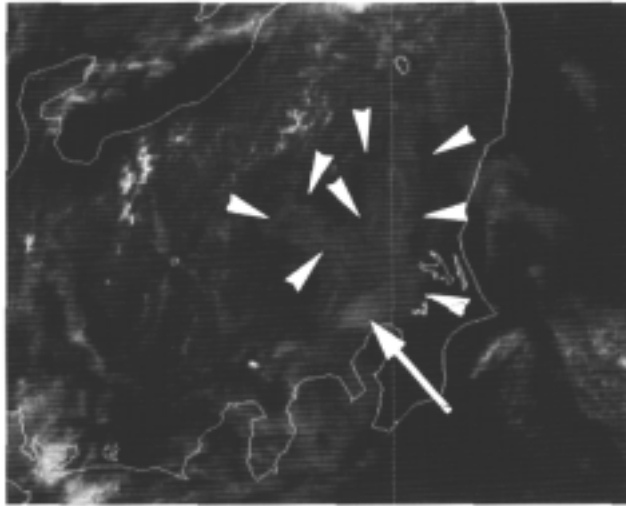


Figure 7-2-2. Visible image at 02UTC, January 17, 1998  
Wedges: Snow cover Arrow: Low cloud

### 7.3 Yellow sand

The yellow sand originates in the yellow soil zone and Gobi Desert in the Chinese continent and moves and diffuses with atmospheric currents. At the beginning of origination, it has a bright gray area with a relatively distinct border on the visible image. By the time when it reaches around Japan, it diffuses and becomes thin, so its identification becomes difficult on the visible image.

On the visible image in Figure 7-3-1 a, a veil-like bright gray region shaded at places is seen from northern to central China on the Asian continent, and it is a yellow sand (marked by wedges). On the infrared image (Figure 7-3-1 b), it appears as a clear white region (marked by wedges).

Figure 7-3-2 a shows the visible image one day after Figure 7-3-1 a. The yellow sand moved from central China to the East China and Yellow Seas and became fairly thin (marked by wedges), so its identification became difficult. On the infrared differential image in Figure 7-3-2 b, however it appears white (marked by wedges).

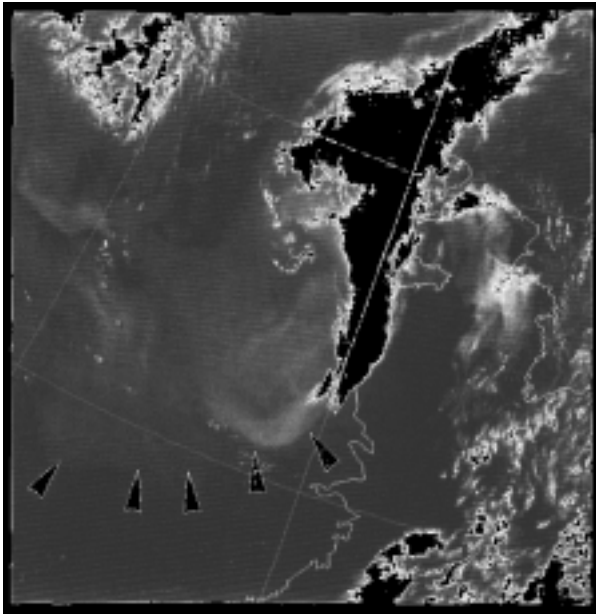


Figure 7-3-1 a.  
Visible image at 06UTC, April 16, 1998  
Wedges: Yellow sand

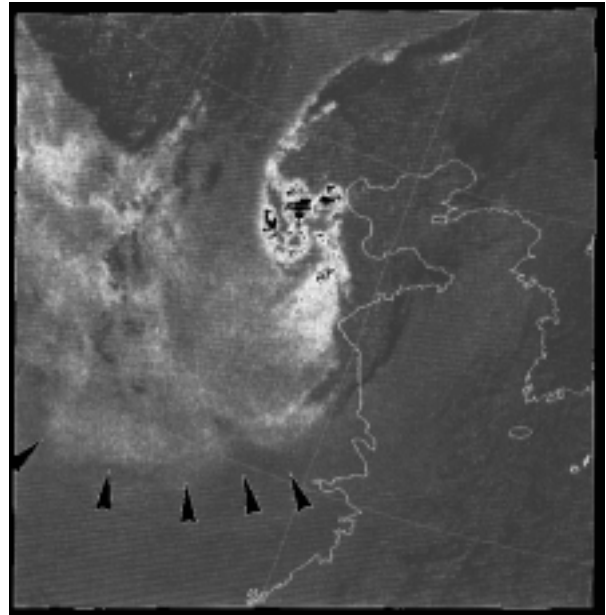


Figure 7-3-1 b.  
Infrared differential image at 06UTC, April 16, 1998  
Wedges: Yellow sand

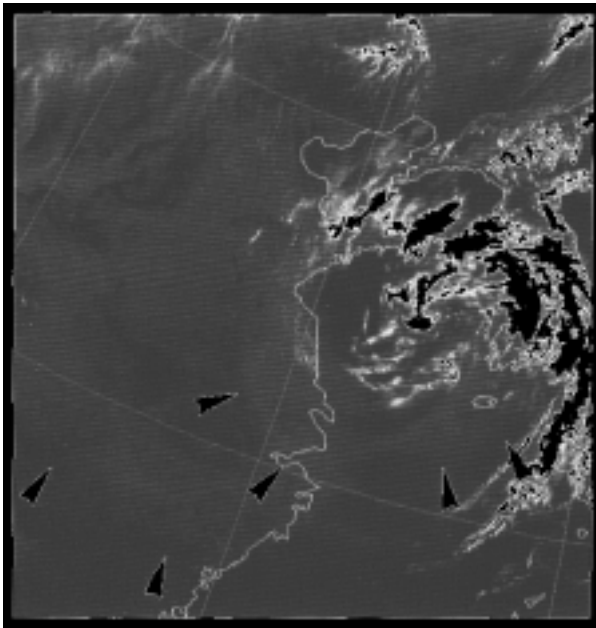


Figure 7-3-2 a.  
Visible image at 06UTC, April 17, 1998  
Wedges: Yellow sand

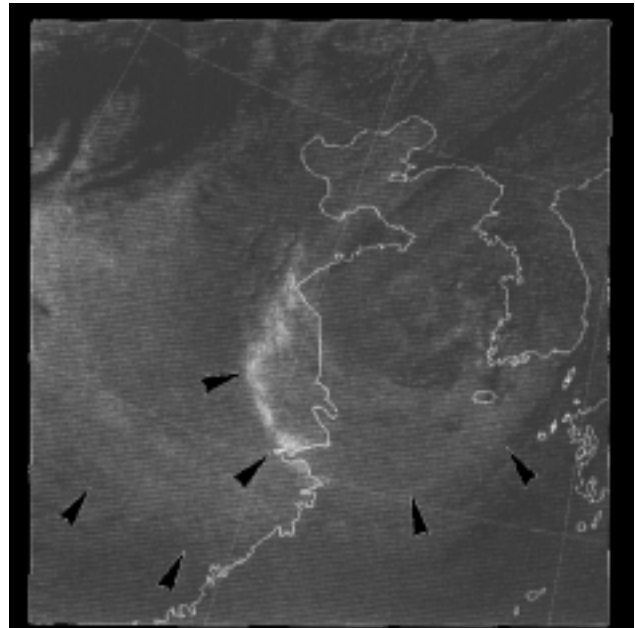


Figure 7-3-2 b.  
Infrared differential image at 06UTC, April 17, 1998  
Wedges: Yellow sand

## 7.4 Volcanic eruption

If a volcano erupts, an intense ascending current is created around the spot of eruption, and this current goes through adiabatic expansion and forms a cloud containing a large amount of volcanic ash. This cloud on the satellite image is circular immediately after the eruption, and it assumes the form of a sector fanning out from the spot of eruption toward the lee as time passes. The sector is narrower and longer for stronger upper-air wind speeds. Detection of this cloud containing volcanic ash is possible on the visible image or the infrared image indeed, however, more distinct detection is possible using the infrared differential image, on which distinction is possible between cloud and volcanic smoke or yellow sand (see Section 1.3.6).

Figures 7-4-1 a and b show an example of eruption of Mt. Bezuimiani and are the infrared image and infrared differential image at 03UTC, October 6, 1995. On the infrared image, distinction from the surrounding clouds is difficult, however, the volcanic smoke is represented in white on the infrared differential image. As time passes to 06 and 09UTC (Figures 7-4-2 and 7-4-3), the volcanic smoke is seen flowing to the east.

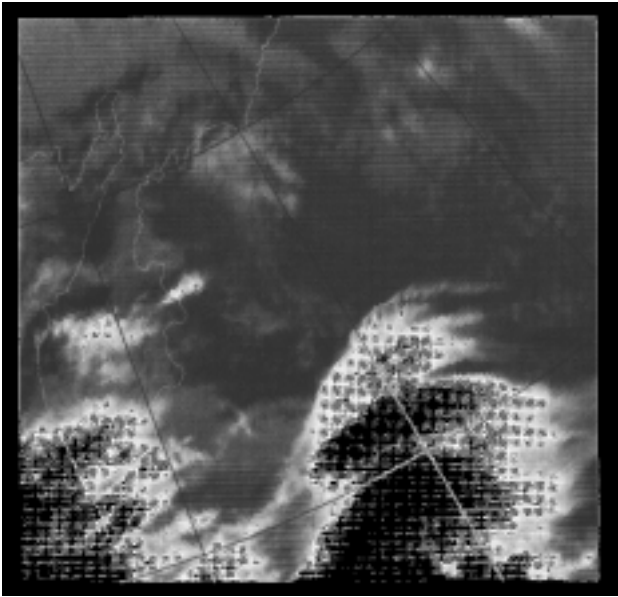


Figure 7-4-1 a. Infrared image at 03UTC, October 6, 1995

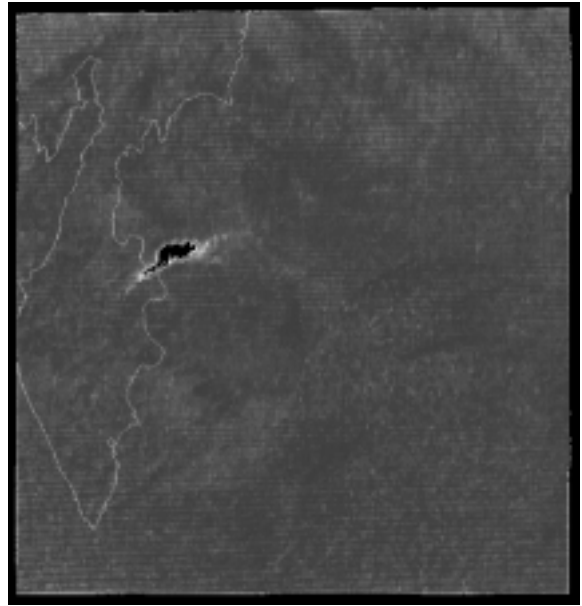


Figure 7-4-1 b. Infrared differential image at 03UTC, October 6, 1995

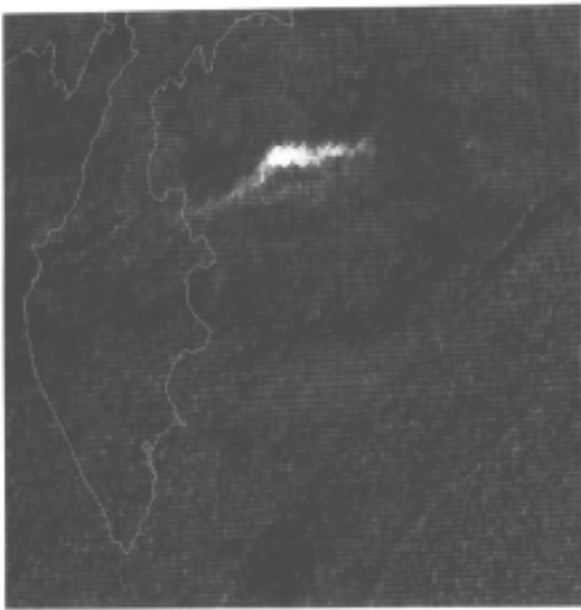


Figure 7-4-1 c. Infrared differential image at 06UTC, October 6, 1995

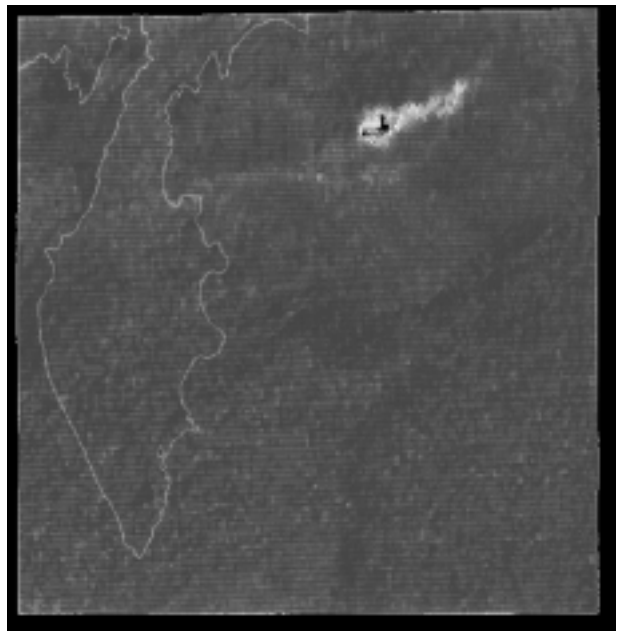


Figure 7-4-1 d. Infrared differential image at 09UTC, October 6, 1995

## 7.5 Forest fire and smoke

Small forest fires are difficult to detect from the satellite image. However, if they grow to a large scale extending over several hundred kilometers and continuing to burn over several weeks, the spot can be identified from the state of the smoke seen on the visible image if there is no cloud. Until the fire is extinguished, the smoke flows with the winds at low levels and drifts around. The smoke drifting around is seen in white and thin veil-like form on the visible image. Because the underlying land or sea can be seen through, distinction from cloud is possible. On the infrared image, a forest fire can be detected as a small region of high temperature (hot spot) (Fuchida and Onozato, 1998).

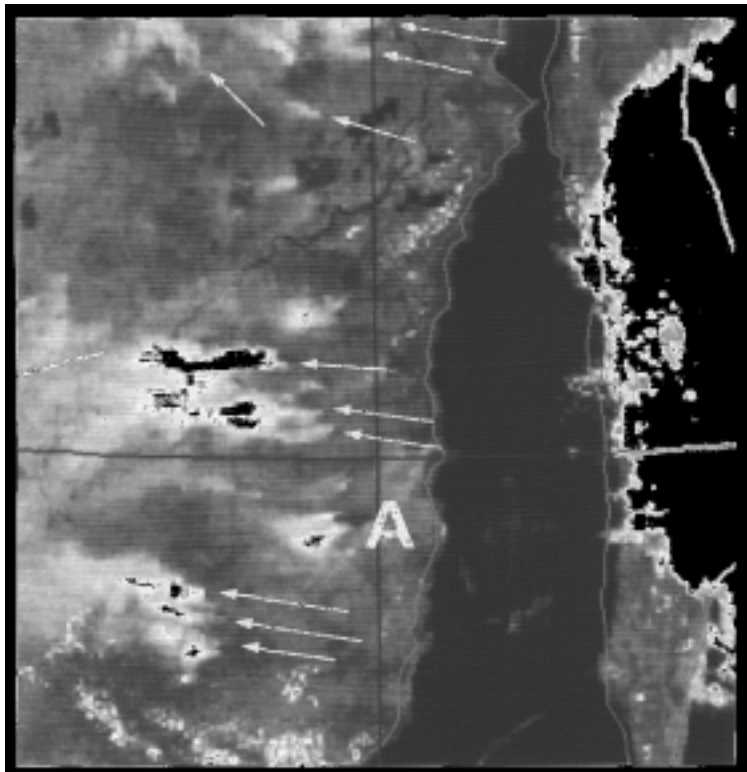


Figure 7-5-1. Visible image at 03UTC, August 7, 1998  
Symbols: Refer to the text.

Figure 7-5-1 shows the visible image at 03UTC, August 7, 1998 with the Maritime Territory magnified. Many white fluffy spots (marked by arrows) are seen. These are smokes flowing out of the origins of fires. Figure 7-5-2 shows a temperature distribution map based on the infrared image at the same time. The root (A) of the white fluffy spots on the visible image agrees well with the region of 20°C or over indicated by (A) on the temperature distribution map. From this, this spot (hot spot) can be estimated to be the origin of the fire.

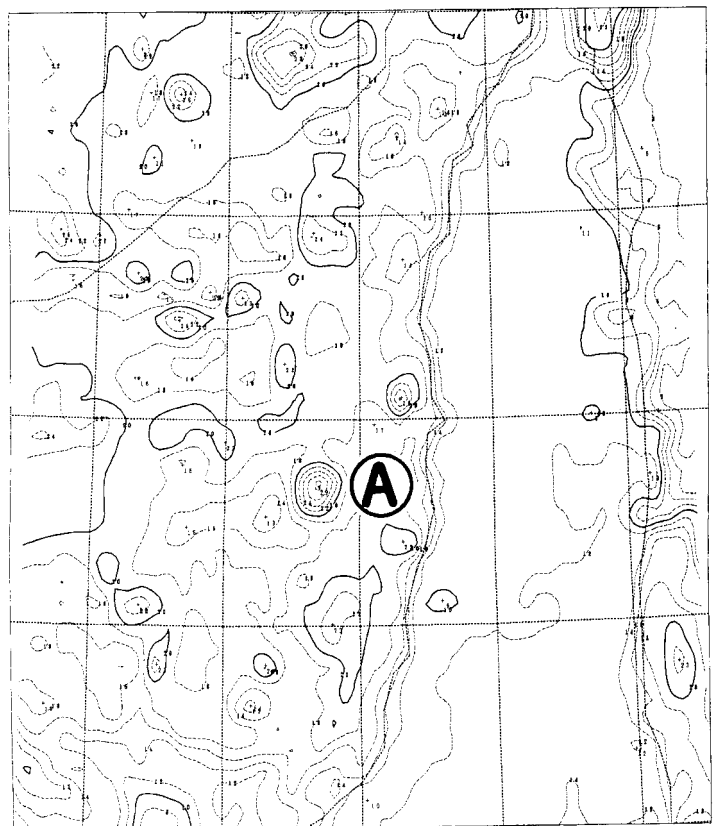


Figure 7-5-2.  
Infrared temperature distribution map at 03UTC, August 7, 1998  
Broken line: 2°C interval Bold line: 10°C interval  
Symbols: Refer to the text.

Figure 7-5-3 shows the smoke of a forest fire that occurred in Indonesia. A smoke indicated bright gray (marked by wedges) can be observed from Borneo to Sumatra. This forest fire occurred for several months from the summer of 1997 at places in Indonesia. The smoke spread over Southeast Asian countries. On the satellite image as well, this smoke was observed over several months.

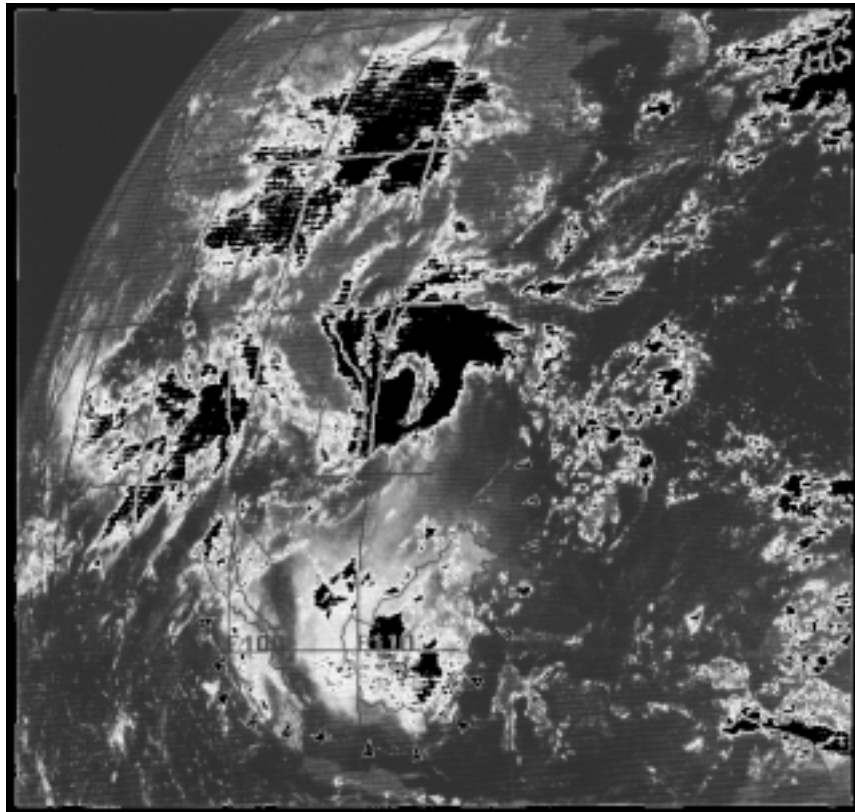
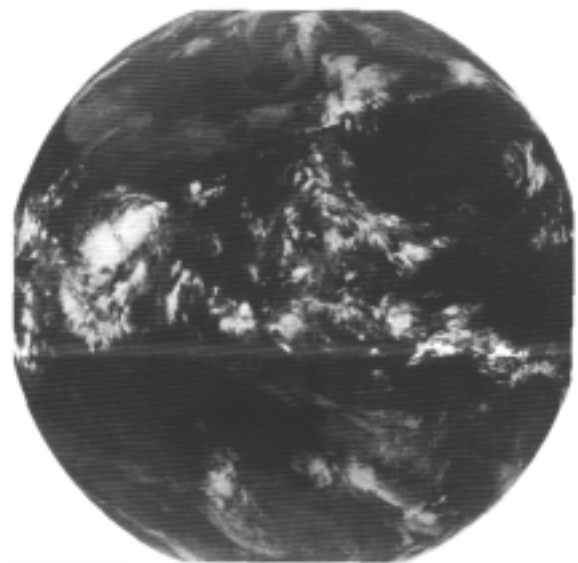


Figure 7-5-3. Visible image at 03UTC, September 23, 1997  
Wedges: Refer to the text.

### Level-down by the moon

For calibration of the infrared image, the temperature of outer space is measured as a body of low brightness at each scan time of the radiometer. If the moon is present in the optical field of observation, the reference value for calibration is shifted and a level-down of the infrared image occurs because the temperature of the moon is higher than outer space. This phenomenon occurs several times a month, but in almost all cases the influence is small. However, an influential level-down may occur depending on the position and the age of the moon. Attached Figure 1 shows the infrared image under such a large influence. A white belt is seen near  $10^{\circ}$  S, and it is due to the influence of a level-down by the moon. (Kazufumi Suzuki)



Attached Figure 1. Level-down by the moon  
(infrared image at 00UTC, October 23, 1999).



## 7.6 Sun glint

Sunlight is reflected from the water surface such as the oceans and large lakes, and this reflecting phenomenon is called sun glint. On the visible image, it appears as a large bright region and its position is depending on season and time of day. The size and intensity of sun glint alters according to the water surface conditions, that is, the sun glint is small and bright for a sea surface not waving under calm winds. On the other hand, if the winds are intense and the sea surface is waving high, the sun glint is large and dark. That is, the sea surface conditions can be known through the sun glint.

Figure 7-6-1 shows the mechanism of sun glint. A calm sea surface acts as a mirror. Sunlight reflected from the sea surface at the point B is directly incident upon the sensor of the satellite. On the other hand, sunlight reflected at the point A is not directly incident upon the sensor of the satellite. That is, the satellite sees directly the sunlight reflected at the point B, which is seen as the brightest region (sun glint) on the visible region. A sun glint moves over the image from east to west within a day. Across the seasons, its center swings between  $11.75^{\circ}$  N and  $11.75^{\circ}$  S.

On the visible image in Figure 7-6-2, the shining region around  $10^{\circ}$  N and  $140^{\circ}$  E (marked by a wedge in the figure) is sun glint. Since this sun glint is small and bright, the sea surface around here can be estimated to be calm. The position of sun glint lies in the northern hemisphere because it was July, and around  $140^{\circ}$  E because the image was taken at noon (Japan Standard Time).

In Figure 7-6-3, the sun glint lies around  $10^{\circ}$  S and  $160^{\circ}$  E (marked by a wedge in the figure). The position of the sun glint is on the southern hemisphere because it was December and around  $160^{\circ}$  E because the image was taken at 900 (Japan Standard Time).

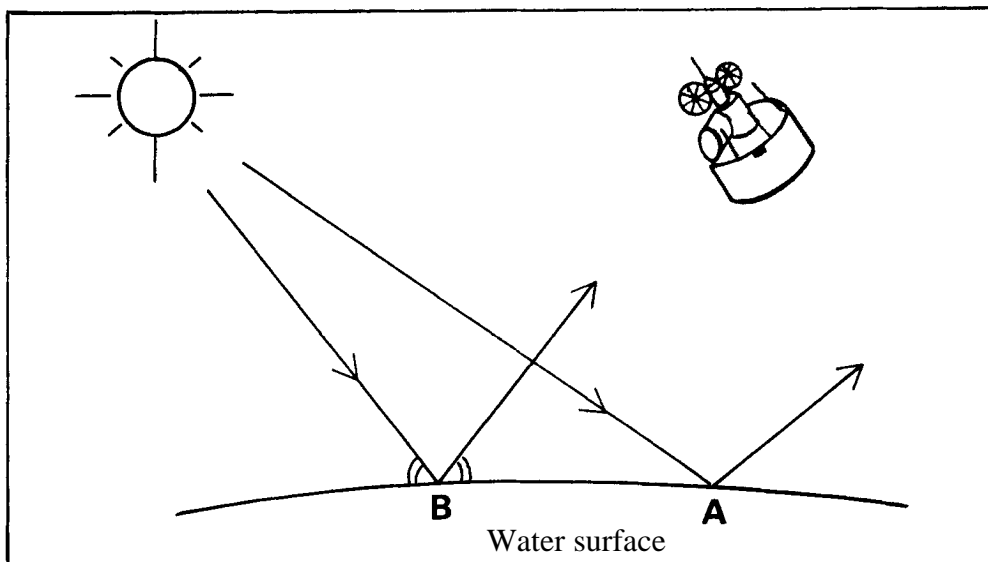


Figure 7-6-1. Mechanism of sun glint  
Arrow with continuous-line shaft: Sunlight Symbols: Refer to the text.

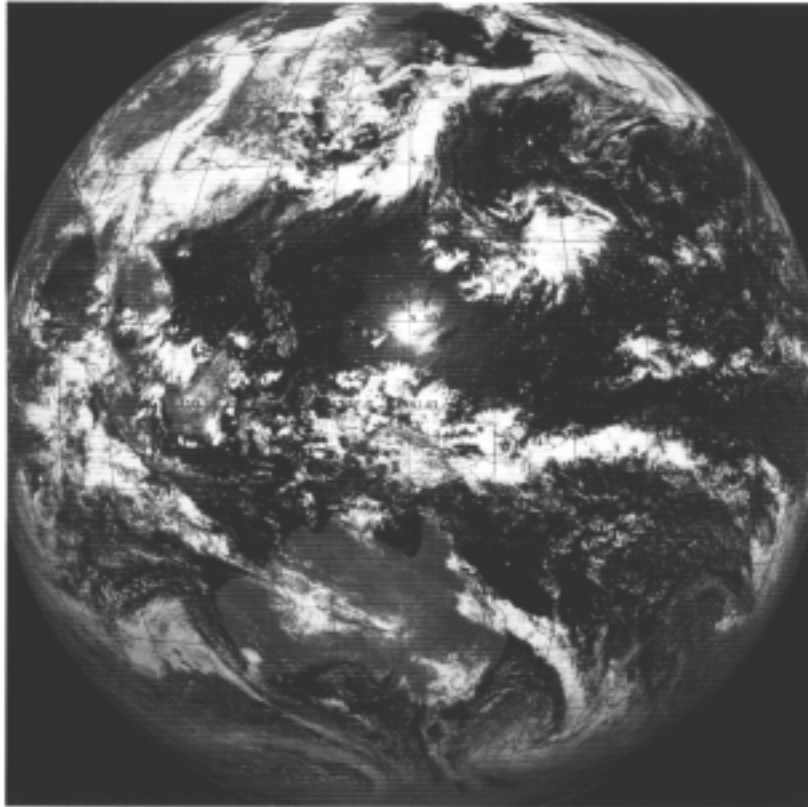


Figure 7-6-2. Visible image at 03UTC, July 22, 1998  
Wedge: Refer to the text.

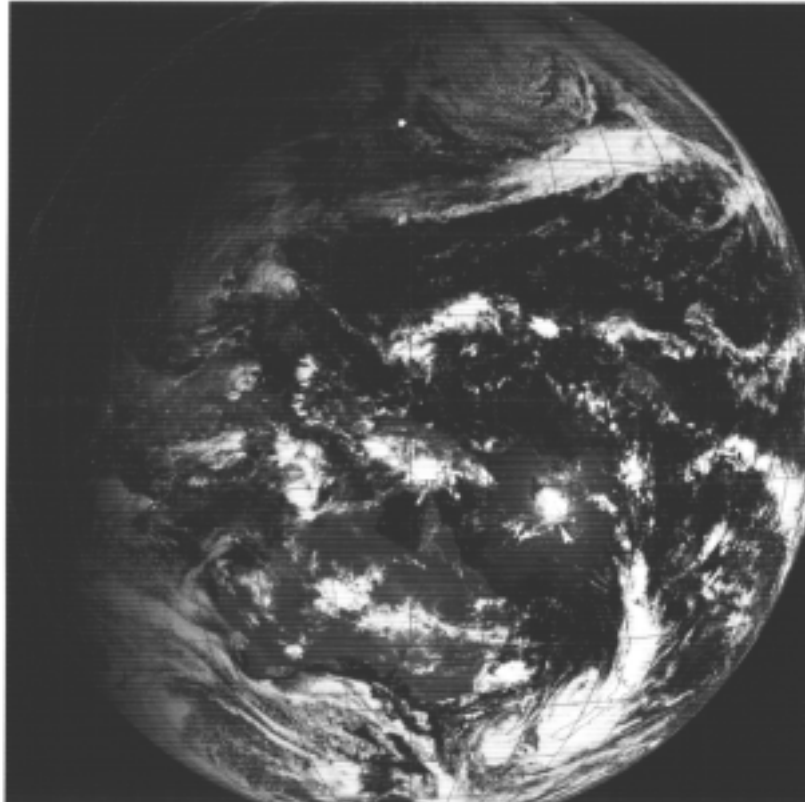


Figure 7-6-3. Visible image at 00UTC, December 18, 1998  
Wedge: Refer to the text.

## 7.7 Shiome (merging area of two tidal currents)

The distinct difference in ocean surface temperature associated with shiome is represented on the infrared image as a slight difference in gray level (marked by wedges). It can be recognized more distinctly if the gray scale of the image is enhanced. Because the sea surface temperature varies little with respect to time, its distinction from cloud is easy by using the moving image. Shiome cannot be seen on the visible image because sea surface temperature variations cannot be captured on the image.

Figure 7-7-1 shows an example of shiome that was seen from the waters south of Hokkaido to the waters east of Kanto. It can be seen that the sea surface temperature is lower as one goes up north. With this gray scale, distinct temperature difference can be seen in the three gray levels of gray, dark gray and black. In particular, a warm water mass (encircled by triangles) 200 to 300 km across in a latitudinal direction with a distinct temperature difference on the northern fringe is seen in black around 40° N off Sanriku.

In the Chart of Sea Surface Temperature around Japan of this month (Figure 7-7-2), a warm water mass (A) of 11°C or higher can be recognized around 40° N off Sanriku, and the temperature gradient is large on the north and south side of this warm water mass. These agree with the shiome in the image.

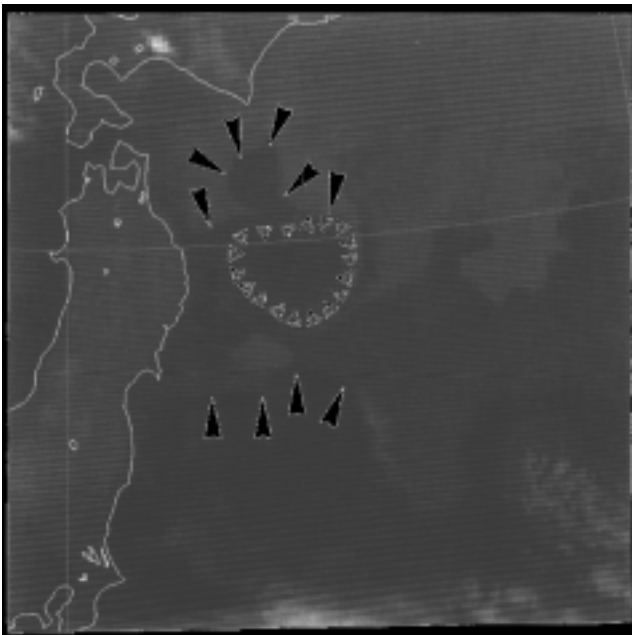


Figure 7-7-1.  
Infrared image at 12UTC, April 9, 1999  
Wedges: Shiome (merging area of two tidal currents)  
Triangle: Warm water mass

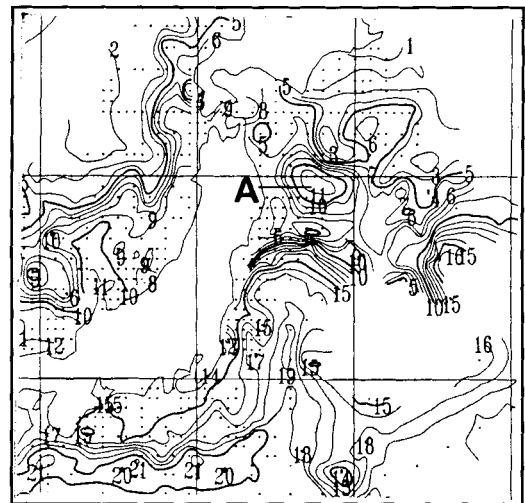


Figure 7-7-2. Chart of Sea Surface Temperature around Japan in April 1999  
Bold line: 5°C interval Thin line: 1°C interval  
•: Observation point Symbols: Refer to the text.

## 7.8 Solar eclipse

The solar eclipse can be observed on the satellite image though it is rare. In Figure 7-8-1, the portion indicated by an arrow is a solar eclipse. There is a darker portion than the surroundings around the arrow in the ocean area east of Japan. This is a shadow of the moon cast onto the earth. To make the shadow of the moon easy to recognize, the portion of the image encircled by a broken line is magnified and enhanced in gradation and is shown in Figure 7-8-2. It appears on a white cloud as a black circle 350 km in diameter centered on about 32° N and 152° E. Around it, the brightness is decreased in circular form, clearly indicating the state of the eclipse.

In contrast to surface observation, clear observation is possible for satellite imagery when clouds are distributed widely because the shadow of the moon is cast onto the clouds.

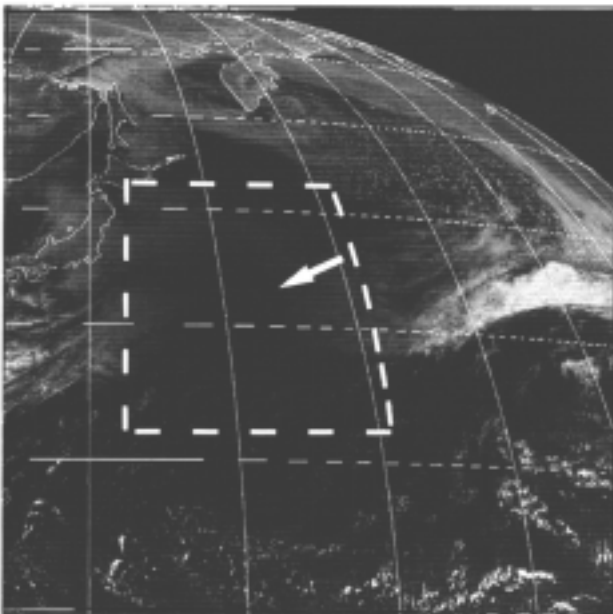


Figure 7-8-1.  
Visible image at 03UTC, March 18, 1988  
Symbols: Refer to the text.

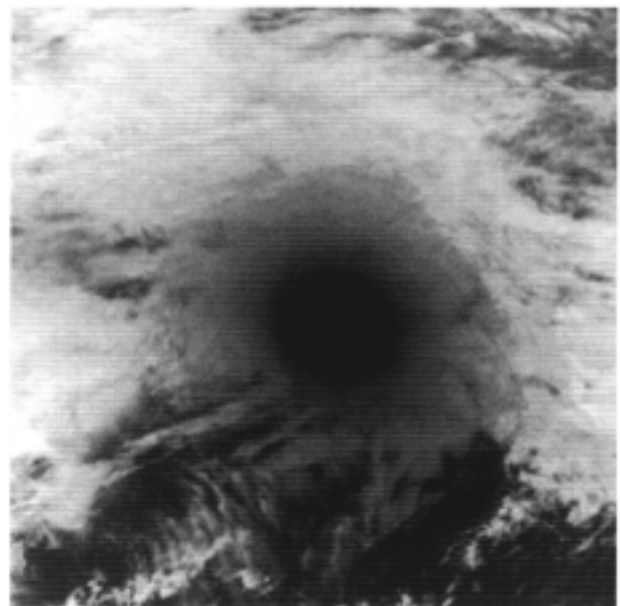


Figure 7-8-2.  
Enhanced visible image at 03UTC, March 18, 1988